

A new Method for parametric BBF generation

Alexandre Jacquemart

Research & Innovation

ESI Group France

Rungis, France

alexandre.jacquemart@esi-group.com


Mokrane Hadj-Bachir

Research & Innovation

ESI Group France

Nantes, France

mokrane.hadj-bachir@esi-group.com


Sio-Song Ieng 

PICS-L, COSYS

Univ Gustave Eiffel

Marne la Vallée, France

sio-song.ieng@univ-eiffel.fr

Dominique Gruyer 

PICS-L, COSYS

Univ Gustave Eiffel

Marne la Vallée, France

dominique.gruyer@univ-eiffel.fr

Abstract—In a large set of applications, belief theory is applied to handle and to manage efficiently uncertainty and conflict. An essential step consists in choosing the appropriate Basic Belief Function (BBF) to generate Basic Belief Assignments (BBA) before the combination stages. In this context, we introduce a novel method that leverages belief theory to generate BBA using a parametric family. This approach offers a structured framework for evaluating objective criteria and selecting the most suitable BBF for a given scenario. The method is designed to accommodate a wide range of applications, from decision-making in uncertain environments to data fusion in complex systems. The key advantage of our method lies in its flexibility and adaptability. By using a parametric family of functions, the method can tailor the BBA generation process to specific requirements, such as the level of noise or discordance in the sources. This allows us to optimize the performance of the fusion architecture and improve decision-making accuracy. Our method was applied to select the most suitable candidate from a set of functions, aiming to minimize the effects of noise and discordance. This involved evaluating the performance of each function against a set of objective criteria, such as robustness and reliability. The results highlighted that our method outperformed existing approaches, demonstrating its effectiveness in generating BBAs that are well-suited to the task at hand. In conclusion, our method offers a new level of adaptability and generality in BBA generation, enabling the customization of hyperparameters to optimize data fusion processes.

I. INTRODUCTION

In today's data-driven world, the fusion of imperfect raw data from disparate sources has emerged as a critical task across a multitude of domains. From healthcare and finance to environmental monitoring and autonomous systems, the effective integration of diverse data streams is essential to extract and gain valuable information for informed decision-making. Various scientific data fusion techniques are available, including data association such as clustering methods, state estimation methods such as Kalman filtering, or Decision estimation methods such as Dempster-Shafer theory (DST).

DST, also known as the evidence theory or belief theory, is a mathematical framework used to model and use uncertain and incomplete information through a set of combination

operators. Nevertheless, to feed these combination rules, it is needed to operate a set of BBA from upstream information by using a BBF. While BBFs have played a pivotal role in data fusion methodologies, there remain significant avenues to improve their applicability and effectiveness within the broader spectrum of fusion techniques. Numerous previous works have already proposed architectures for fusing data using DST, such as [1], [2], [3], and [4]. Another approach in DST data fusion is to define an optimizable framework and then approximate a BBF to resolve the problem. This field, pioneered by [5], was iterated in works like [6] and [7].

Improvements in DST include refining conflict management methods to ensure more accurate estimations when dealing with conflicting information sources [8], [9], [10], [11]. Specific fields, like healthcare [12], finance [13], and security [14], also takes benefice from the uncertainty modeling and use, despite each having its own unique requirements for handling it and merging data. These advancements have a direct impact on how BBFs and BBAs are managed within DST.

In this paper, we propose a generic methodology to generate parameterized families of functions for BBF generation and show that we can define and use objective criteria to find the most suitable parameters, here namely the acceptance and refutation function. In the second section, we will present an overview of the DST domain. Then, the mathematical framework is presented in the section III. This framework is then applied to find the best set of functions to minimize the impact of noise and discordance of multiple information sources, in section IV. Finally, we conclude and propose ways of improvement in section V.

II. BACKGROUND

A. Evidence theory

Evidence theory, widely known as Dempster-Shafer theory, provides a systematic framework for modeling uncertainty and handling inaccurate information. The theory was first introduced by Dempster in [1], and later formalized by Shafer in [15]. At its core, the theory revolves around the concept

of Basic Belief Functions (BBFs), which quantify the degree of belief assigned to different propositions. This framework excels in scenarios where evidence is incomplete, conflicting, or characterized by ambiguity. However, traditional BBFs may lack the adaptability required to address specific challenges.

The mathematical underpinning of evidence theory lies in the calculation of belief masses, which represent the degrees of belief associated with various propositions. Let 2^Ω denote the power set of the frame of discernment Ω , representing all possible subsets of Ω . A Basic Probability Assignment (BPA), denoted by m , assigns a belief mass to each possible subset of Ω . Formally, $m : 2^\Omega \rightarrow [0, 1]$, and it satisfies two key conditions:

- Normalization: $\sum_{A \subseteq \Omega} m(A) = 1$.
- Dempster's rule : For any disjoint $A, B \subseteq \Omega$, the combined belief mass for $A \cup B$ is given by $m(A \cup B) = \sum_{C \subseteq A \cap B} m(A \cap C) \cdot m(B \cap C)$.

The Dempster's rule allows the combination of evidence from different sources, even when the sources are not in agreement. This merging of evidence is crucial in situations where uncertainty and conflicting information are prevalent.

B. Formal system of logic

A formal system of logic is a structured framework governed by rules describing the combination of axioms, with symbols representing logical components such as propositions, variables, connectives (e.g., "and," "or," "not"), and quantifiers (e.g., "for all" and "there exists"). These rules of inference facilitate the valid manipulation and combination of symbols, ensuring logical soundness and adherence to established principles of validity. Axioms, fundamental to formal logical systems, serve as self-evident truths or basic principles upon which deductions are built, providing starting points for deriving further logical truths through deductive reasoning. In essence, formal logic provides an accurate and systematic methodology for analyzing and evaluating arguments across diverse disciplines, including mathematics, philosophy, computer science, and linguistics.

In the field of evidence theory, three fundamental assumptions guide the interpretation and reasoning about information: The Closed-World Assumption (CWA), the Open-World Assumption (OWA), and the Extended Open World Assumption (EOWA).

- The CWA posits that the frame of discernment is completely known or completely unknown. Under this assumption, any information not explicitly provided is considered false. Any uncertainty is considered as an uncertainty on which hypothesis in this frame of discernment the tested assertion falls under.
- The OWA acknowledges a partially known frame of discernment. This framework recognizes that hypotheses may be incomplete, with assertions unsupported by evidence labeled as unknown.
- The EOWA is an iteration of the OWA wherein the uncertainty regarding the completeness of the frame of

discernment, i.e., the existence of an out-of-bound new hypothesis, differs from the uncertainty regarding which hypotheses the tested assertion falls under.

These assumptions provide a structured framework for reasoning about uncertain information in evidence theory, ensuring coherence and effectiveness in the interpretation and utilization of evidence.

III. THE METHOD

In this section, the following notation will be used :

- H_η represents the hypothesis $\# \eta$ being True
- \bar{H}_η represents the hypothesis $\# \eta$ being False
- Ω represents the uncertainty on which hypothesis to choose
- H_* represents the uncertainty on the completeness of the frame of discernment (EOWA)

A. Definition and formulation of a novel BBA family

One of the problems with data and sensor fusion is to establish a link between two objects x , y , or two sets X and Y of objects x_i and y_j , $i = 1, \dots, n, j = 1, \dots, m$ for example a multi-object tracking system: X is the set of n perceived objects by sensors and AI algorithm and Y is the m known tracks. The decision system, following the output of different sources, must provide an answer to the question : "Is the perceived object by the AI system x_i in relation with the known track y_j ?" This question can be simplified with the notation $X \mathfrak{R} Y$ is true or false? Thus, the decision is thus to determine if the relation $X \mathfrak{R} Y$ is true or not. One solution to match two objects is to compute a similarity metric d_{ij} such as Mahalanobis distance or Jaccard index. The drawback of only using this kind of similarity metrics is usually not enough to handle the different attributes that can describe the objects. The DST is the well-known theory to handle the different attributes and conflicts that might appear. The DST assigns a belief mass to each element of the power set, as it is explained in section II-A. However, the difficult in the theory is that the BBA depends on the application field and there is so far not yet general methodology to generate appropriate Basic Belief Function (BBF). The BBF is a function whose definition domain is the similarity or dissimilarity set S and the codomain is $[0, 1]$. Using for instance a normalized S such as Jaccard Index, $S = [0, 1]$. In the framework of object association $X \mathfrak{R} Y$, a mass distribution with three components of hypothesis must be used, as presented in the section II-B.

In our method, the BBF is based on a chosen function f which must verify the continuity and derivability constraint on a real interval $[a, b]$ where a and b are real and $b > a$. As an example, in [16], a sinusoidal function is proposed for the multiple vehicles tracking. In our framework, any function can be selected to solve a given fusion problem. The continuous and derivability constraints are a critical property for the function family generation and the optimal BBA selection that will be detailed in the following sections. Two transformations on f are applied, so that the resulting operator $Gf(\cdot)$ is defined

in the interval $[0, 1]$ and the codomain of $Gf(\cdot)$ is $[0, 1]$. The operator $G(\cdot)$ is defined as follows:

$$Gf(x) = \frac{f((b-a)x+a) - \min(f)}{\max(f) - \min(f)}. \quad (1)$$

The results of these transformations can be seen in Fig. 1. These initial transformations involve scaling the given f along both the abscissa and ordinate axes. Consequently, the focus is on the shape and variations of the curve. When analyzing the shape and variations of a curve, we examine how it behaves and evolves in relation to its independent and dependent variables. This may involve studying how the curve slopes or curves, whether it exhibits symmetry or asymmetry, and how it responds to variations in its input parameters. By preserving the shape and variations of the curve, our objective is to capture the evolving patterns within the information sources.

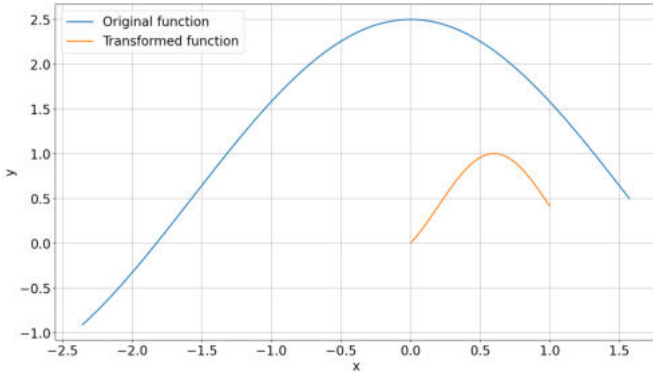


Fig. 1. Plot of the different transformations applied to $f(x) = 2\cos(x) + 0.5$ on $[-\frac{3\pi}{4}, \frac{\pi}{2}]$. The blue curve is the original one, whereas the orange curve is the curve after applying the operator G .

To solve the conflict problem, we apply the same constraints of [17]:

- The perceives object x_i is in relation with no more than one track y_j .
- The known track y_j is in relation with no more than one perceived object x_i .

To meet these constraints, [2] introduced two parameters τ_1 and τ_2 . However, only one parameter τ can be used by assuming $\tau_1 = \tau_2$. τ separates the normalized dissimilarity interval $S = [0, 1]$ into two sub intervals.

Depending on the scenario (dissimilarity or similarity), the meaning of the two intervals carries opposite meaning :

- In the case of a dissimilarity metric d_{ij} , the first sub interval $[0, \tau[$ is the support of the mass measuring the dissimilarity between x_i and y_j and where the two objects can be associated. That is, the hypothesis $H = X\mathfrak{A}Y$ can be true (2). The second interval $[\tau, 1]$ represents the area where \bar{H} can be true (3).
- In case of a similarity metric \mathcal{C}_{ij} , the opposite occurs : the first sub interval $[0, \tau[$ is the support of the mass measuring \bar{H} while the second interval $[\tau, 1]$ carries the mass on H .

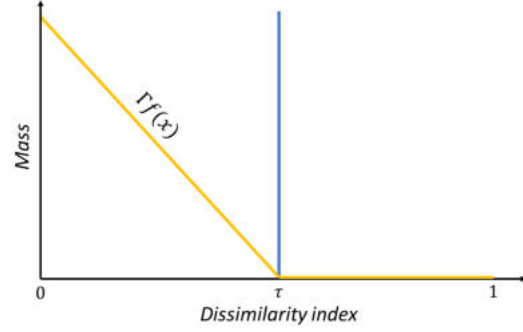


Fig. 2. The parameter τ separates the normalized dissimilarity interval $S = [0, 1]$ into two sub intervals. $[0, \tau[$ is the support of the mass measuring the dissimilarity and in the second, the mass equals 0. Here, $f(x) = -x$ on the interval $[0, 1]$

With the operator G , we define the function family in Eq.2 and 3. Let Γ denote this family, and let f be a function that satisfies the properties described earlier. Then, for all $\tau \in [0, 1]$:

$$\Gamma_f(x) = \begin{cases} Gf(\frac{x}{\tau}) & x < \tau \\ 0 & x \geq \tau \end{cases} \quad (2)$$

$$\bar{\Gamma}_f(x) = \begin{cases} 0 & x \leq \tau \\ Gf(\frac{1-x}{1-\tau}) & x > \tau \end{cases} \quad (3)$$

Γ_f will be termed a *collapsible function of f on τ* . This parametrisation allows us to regulate, through the parameter τ , the threshold at which the source is considered meaningful or meaningless while preserving the dynamic of the basic function for increasing or decreasing belief mass. Depending on the quantity under study, either $\Gamma_f(x)$ or $\bar{\Gamma}_f(x)$ can be used, depending on whether the experiment uses similarities or dissimilarities metrics.

B. Generating a dichotomic set of mass using the previously defined function family

Let's consider a pair of functions, denoted as *acc* and *ref*, which satisfy the prerequisites to be used in $G(\cdot)$. Here, *acc* is referred to as the acceptance function, while *ref* is termed the refutation function. Given a single input value x , two dichotomic sets of mass are available, depending on the expected behavior of x . In both cases, the Basic Belief Function (BBF) is defined as follows:

$$m_{\Gamma(\cdot)} = \begin{bmatrix} m_{\Gamma}(H) \\ m_{\Gamma}(\bar{H}) \\ m_{\Gamma}(\Omega) \end{bmatrix} \quad (4)$$

$m_{\Gamma_f}(H)$ is the mass relative to the belief of the hypothesis being true and is a function of *acc*. $m_{\Gamma}(\bar{H})$ is the mass relative to the belief of the hypothesis being false and is a function of *ref*. $m_{\Gamma}(\Omega)$ represents the mass of ignorance. $m_{\Gamma}(H)$ and $m_{\Gamma}(\bar{H})$ are defined from Γ_f and $\bar{\Gamma}_f$. Concerning $m_{\Gamma}(\Omega)$, it is defined using the property of the sets of mass : $m_{\Gamma}(H) +$

$m_\Gamma(\bar{H}) + m_\Gamma(\Omega) = 1$, that leads to $m_\Gamma(\Omega) = 1 - m_\Gamma(H) - m_\Gamma(\bar{H})$

Additionally, drawing from [18], a new parameter $\alpha \in [0, 1]$ is introduced. This parameter is known as the confidence coefficient (or attenuation coefficient) of the source, weighs the masses of hypotheses and represents a degree of confidence in the source.

In the dissimilarity context, that is, x approaches 0 means a stronger belief in the hypothesis, $m_\Gamma(\cdot)$ is defined as followed :

$$m_\Gamma(\cdot) = \begin{bmatrix} m_\Gamma(H) \\ m_\Gamma(\bar{H}) \\ m_\Gamma(\Omega) \end{bmatrix} = \begin{bmatrix} \alpha \cdot \Gamma_{acc}(x) \\ \alpha \cdot \overline{\Gamma_{ref}}(x) \\ 1 - \alpha \cdot \Gamma_{acc}(x) - \alpha \cdot \overline{\Gamma_{ref}}(x) \end{bmatrix} \quad (5)$$

On the other hand, in the similarity context, that is, $x \rightarrow 1$ signifies stronger belief in the hypothesis, the BBF is defined as :

$$m_\Gamma(\cdot) = \begin{bmatrix} m_\Gamma(H) \\ m_\Gamma(\bar{H}) \\ m_\Gamma(\Omega) \end{bmatrix} = \begin{bmatrix} \alpha \cdot \overline{\Gamma_{acc}}(x) \\ \alpha \cdot \Gamma_{ref}(x) \\ 1 - \alpha \cdot \overline{\Gamma_{acc}}(x) - \alpha \cdot \Gamma_{ref}(x) \end{bmatrix} \quad (6)$$

IV. EXPERIMENTS

The experiment introducing our mass function aims to identify the most effective function for mitigating noise and information loss in fusion processes. To accomplish this, N virtual sources, each expressing themselves across \mathcal{H} hypotheses with probabilities, are simulated. A uniform noise sample for an interval $[0, \Delta]$, $\Delta \in [0, 1]$ is then applied. Finally, the data are merged using fusion operators. For convenience, let's denote $S = 1..N$ and $\mathcal{W} = 1..\mathcal{H}$.

A. The fusion architecture

Drawing from the works of [2], two fusion operators are adopted: the "Shared Hypothesis Experts Combination Operator" (or "Multi-Criteria Fusion") and the "Self-assessing Experts Combination Operator" (or "Multi-Object Fusion"). The experiment is to replace their fixed BBF (Eq. 11-15 in [2]) with m_Γ and see which function is the most suitable for the defined purpose. Fig. 3 is a schematic vision of the entire architecture.

Firstly, the sources, in the experiments, are virtual and simulated. The parameters and the mechanic of such sources of information are drawn in IV-B. Each source outputs \mathcal{H} probabilities, one for each hypothesis. Using sources parameters and m_Γ , those sources are processed instantly into \mathcal{H} sets of mass $m_\Gamma^{i,\eta}(\cdot)$, $i \in S, \eta \in \mathcal{W}$. Since the probabilities increase when a hypothesis becomes more likely, $m_\Gamma^{i,\eta}(\cdot)$ is given by Eq.6. To compare our method to others, we will draw from [2], since γ_f applied to \sin between $[-\pi/2, \pi/2]$ gives the same BBF, and [18]'s 2 BBF. The latter will be noted *App1* and *App2*. Eq.7 and Eq.8 show the equations of these BBF. The output is

$S \times \mathcal{H}$ triplets of mass as defined in Eq.4, qualified by source and hypothesis number.

$$App1(\cdot) = \begin{bmatrix} m(H) \\ m(\bar{H}) \\ m(\Omega) \end{bmatrix} = \begin{bmatrix} 0 \\ \alpha \cdot (1 - x) \\ 1 - \alpha \cdot (1 - x) \end{bmatrix} \quad (7)$$

$$App2(\cdot) = \begin{bmatrix} m(H) \\ m(\bar{H}) \\ m(\Omega) \end{bmatrix} = \begin{bmatrix} \alpha \cdot x \\ \alpha \cdot (1 - x) \\ 1 - \alpha \end{bmatrix} \quad (8)$$

The second stage of the architecture consists of the Multi-Criteria Fusion operator. This operator processes the sets of masses of all sources on each hypothesis η , producing a single set of masses $m_{1..N}^\eta$ (or m_S^η), as defined in Eq. 9. This operator operates on the CWA. The output is composed of \mathcal{H} sets of mass, as described in the previously referred equation.

$$\begin{aligned} m_S^\eta(\cdot) &= \begin{bmatrix} m_S(H_\eta) \\ m_S(\bar{H}_\eta) \\ m_S(\Omega_\eta) \\ m_S(\emptyset_\eta) \end{bmatrix} \\ &= \begin{bmatrix} \prod_{s \in S} (1 - m_\Gamma^s(\bar{H}_\eta)) - \prod_{s \in S} m_\Gamma^s(\Omega_\eta) \\ \prod_{s \in S} (1 - m_\Gamma^s(H_\eta)) - \prod_{s \in S} m_\Gamma^s(\Omega_\eta) \\ \prod_{s \in S} m_\Gamma^s(\Omega_\eta) \\ 1 - \prod_{s \in S} (1 - m_\Gamma^s(\bar{H}_\eta)) - \prod_{s \in S} (1 - m_\Gamma^s(H_\eta)) \\ \quad + \prod_{s \in S} m_\Gamma^s(\Omega_\eta) \end{bmatrix} \\ &= \begin{bmatrix} 0 & 1 & -1 & 0 \\ 1 & 0 & -1 & 0 \\ 0 & 0 & 1 & 0 \\ -1 & -1 & 1 & 1 \end{bmatrix} * \begin{bmatrix} \prod_{s \in S} (1 - m_\Gamma^s(H_\eta)) \\ \prod_{s \in S} (1 - m_\Gamma^s(\bar{H}_\eta)) \\ \prod_{s \in S} m_\Gamma^s(\Omega_\eta) \\ 1 \end{bmatrix} \quad (9) \end{aligned}$$

The final stage of the architecture is the Multi-Object Fusion operator. This operator processes all sets of masses across all hypotheses and generates a set of masses $m_{1..\mathcal{H}}(\cdot)$ (or $m_{\mathcal{W}}(\cdot)$) encompassing all hypotheses, as defined in Eq. 10. This operator operates within the EOWA. The EOWA is a choice, as this stage can be performed in both CWA, OWA, and EOWA. Originally, the EOWA was chosen to take into account new targets detected. We decided to keep this choice, as the opportunity to monitor a failure induced by a previously unknown hypothesis is appealing. Therefore, the output is

composed of $\mathcal{H} + 3$ masses.

$$m_{\mathcal{W}}(\cdot) = \begin{bmatrix} m_{\mathcal{W}}(H_1) \\ m_{\mathcal{W}}(H_2) \\ \dots \\ m_{\mathcal{W}}(H_{\mathcal{H}}) \\ m_{\mathcal{W}}(H_*) \\ m_{\mathcal{W}}(\Omega) \\ m_{\mathcal{W}}(\emptyset) \end{bmatrix}$$

$$\begin{cases} m_{\mathcal{W}}(H_i) &= m_S(H_i) \cdot \prod_{\eta \in \frac{\mathcal{W}}{\{i\}}} (m_S(\overline{H}_{\eta}) + m_S(\Omega_{\eta})), \forall i \in \mathcal{W} \\ m_{\mathcal{W}}(H_*) &= \prod_{\eta \in \mathcal{W}} (m_S(\overline{H}_{\eta})) \\ m_{\mathcal{W}}(\Omega) &= \prod_{\eta \in \mathcal{W}} (m_S(\overline{H}_{\eta}) + m_S(\Omega_{\eta})) - \prod_{\eta \in \mathcal{W}} (m_S(\overline{H}_{\eta})) \\ m_{\mathcal{W}}(\emptyset) &= 1 - \prod_{\eta \in \mathcal{W}} (m_S(\overline{H}_{\eta}) + m_S(\Omega_{\eta})) - \sum_{\eta \in \mathcal{W}} m_{\mathcal{W}}(H_{\eta}) \end{cases} \quad (10)$$

B. The virtual sources

For this experiment, virtual sources will be utilized, each characterized by the following parameters:

- α : the reliability coefficient of the source
- τ : The extinction parameter
- $P_1, P_2, \dots, P_{\mathcal{H}}$: The probabilities provided by the source for each hypothesis.

In the context of the experiment, the sources are bundled into 2 groups :

- Concordant sources : Those sources share the same parameters, but each of the sources is degraded independently of the other. The hypothesis they will target is the looked after hypothesis. They correspond to multiple independent iterations of the same sources (i.e., Classification algorithm).
- Discordant sources : Those sources are duplicates from a single source. The hypothesis this original source will target is not the one looked after. This corresponds to a single source feeding multiple times of the architecture.

The "duplication" strategy for discordant sources is to be investigated as the multi-criteria fusion operator is not an idempotent operator, and as such, duplicating sources has greater impact on the fusion operator than adding independent sources.

C. Protocol

Experiment parameters include:

- \mathcal{H} : A number of hypotheses
- H_i : The target hypothesis
- N_C concordant sources on hypothesis H_i
- $acc(x)$: An acceptance function, with bounds a_{acc}, b_{acc} .
- $ref(x)$: A refutation function, with bounds a_{ref}, b_{ref} .
- Δ_STEP : a step size to increase the noise. It is used to increase the noise Δ from 0 to 1
- N_REPEAT : the number of repetitions for each step. Since the noise is randomly sampled, N_REPEAT is a parameter that enables us to use statistical measure

to extract general behaviors, and limit improbable noise samples.

The protocol to generate the data is:

- 1) Process $acc(x)$ and $ref(x)$ into $\Gamma_{acc}(x), \Gamma_{ref}(x)$
- 2) Initialize N_C sources on hypothesis N_i with same parameters
- 3) For N_D in $[0, 1, \dots, N_C]$:
 - a) Initialize $\Delta = 0$
 - b) While $\Delta \leq 1$:
 - i) Repeat N_REPEAT times:
 - A) Generate N_C vectors according to concordant sources probabilities parameters
 - B) Sample N_C random noises vector with each values between 0 and Δ
 - C) Add each noise vector to the corresponding vector, those noised vectors represent the noised input from the concordant sources
 - D) Generate a single vector using the probabilities parameters from the discordant source
 - E) Sample a single random noise vector with each value between 0 and Δ
 - F) Add the noise vector to the original vector. The result vector is the noised original input from the discordant sources
 - G) Copy this discordant noise vector N_D times. This generates the discordant sources' input
 - H) Transform each noised probabilities vector into sets of mass using Eq.6
 - I) Perform Multi-criteria fusion as described in Eq.9
 - J) Perform Multi-object fusion as described in Eq.10
 - K) Save the output
 - ii) Compute the mean and standard deviations from the previously saved value.
 - iii) The noise Δ is updated: $\Delta \leftarrow \Delta + \Delta_STEP$.
 - c) From the previously computed mean, compute the score, defined in Eq.11, of the architecture for N_D discordant sources
- 4) Plot the curve of score on the number of discordant sources

An example was carried out with the function x^2 in Fig. 4, with 10 coherent sources on hypothesis 2 and no discordant sources. The 2 first lines represent the mean mass and standard deviation for each of the masses ($H_1, H_2, H_3, H_*, \Omega, \emptyset$). The 3rd line is a plot of all mean curves on the same graph, allowing us to see which mass predominates. As for the last line, it is a representation of the mass function m_{Γ} . A drop of mass on the target hypothesis is noticeable as the noise increases, first trading mass for ignorance, then trading mass for conflict.

D. Objective measure of robustness

As seen in Fig.4, the mass on the target hypothesis is supposed to decreased when the noise increases, denoting

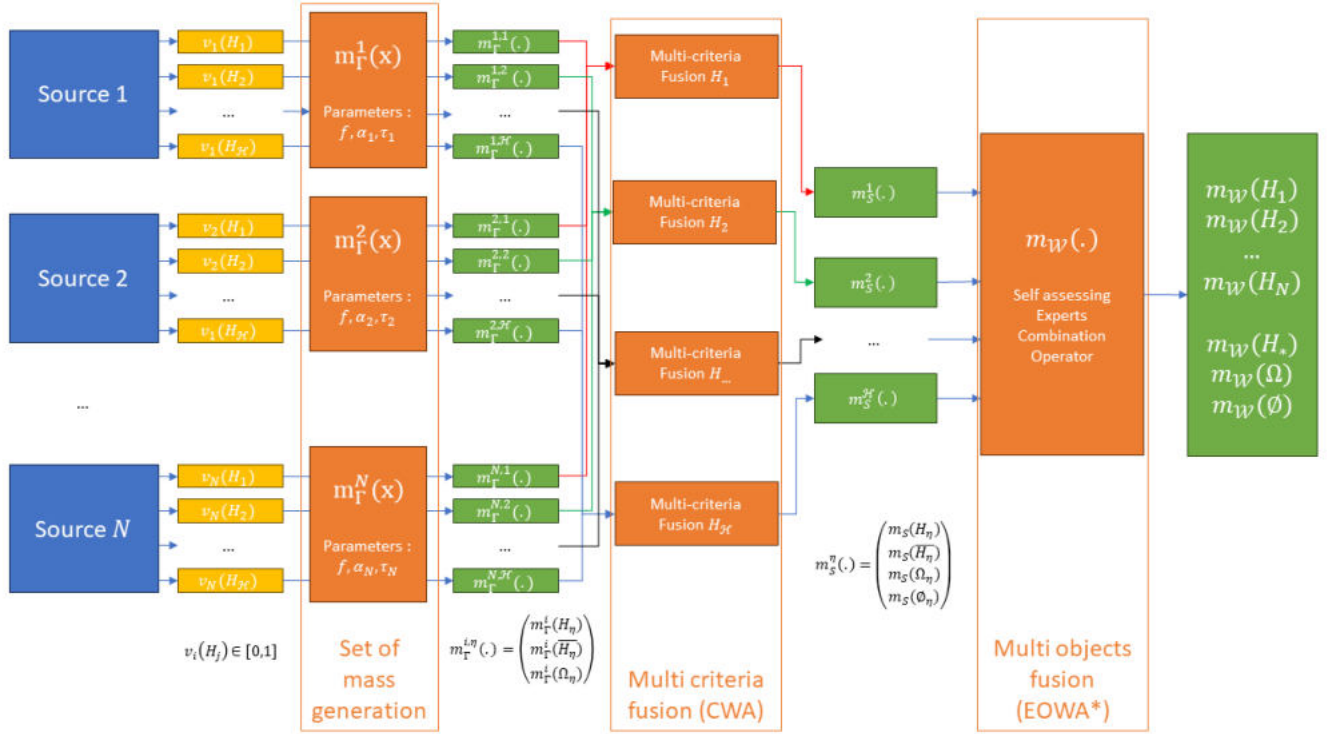


Fig. 3. Fusion architecture for integrating probabilities from N sources across \mathcal{H} hypotheses. The EOWA choice is described later in this paper.

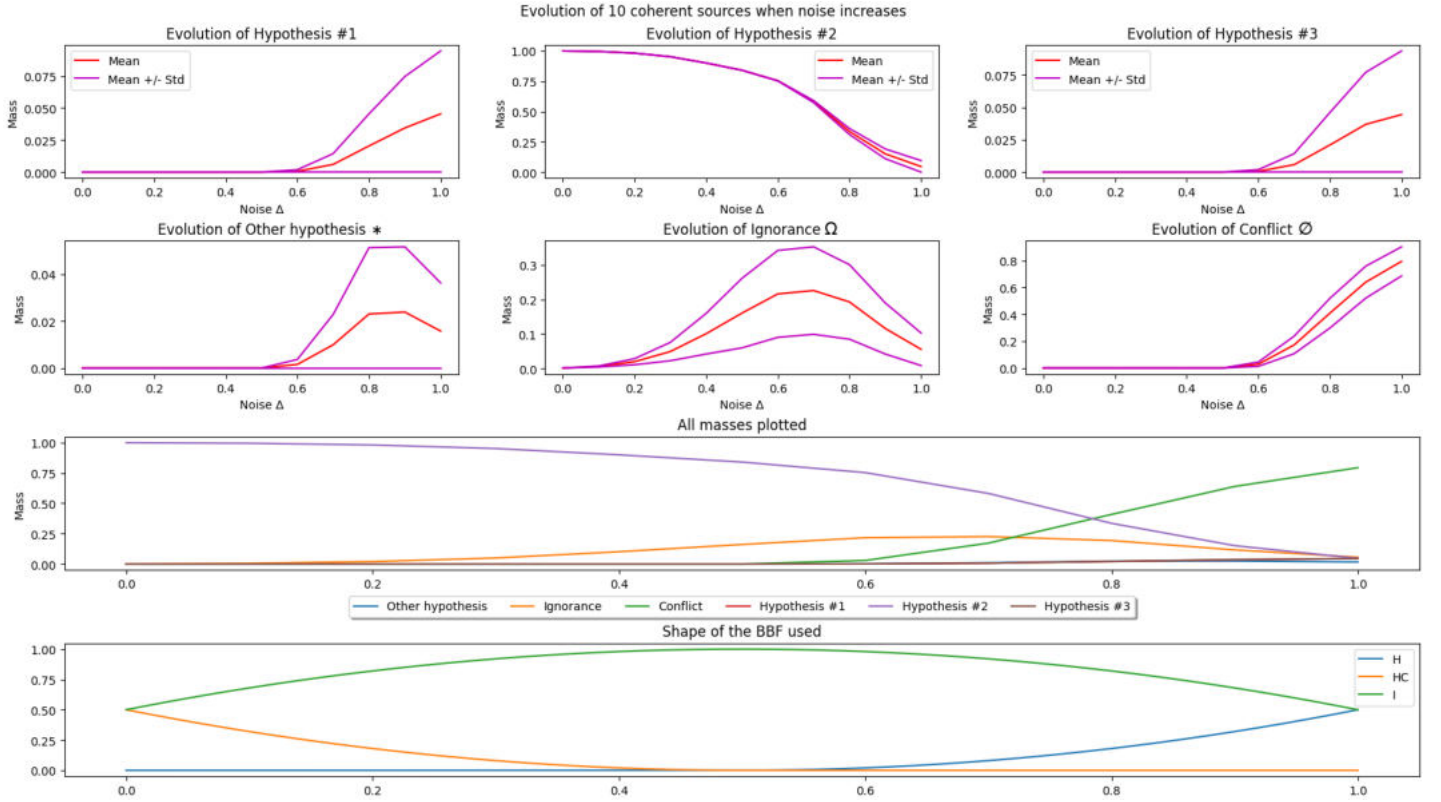


Fig. 4. Plot of the experiment carried out with $(x) = x^2, x \in [-1, 0], ref(x) = x^2, x \in [0, 1]$, probabilities = $[0, 1, 0]$, $\alpha = 0.5$ and $\tau = 0.5$. $\Delta_STEP = 0.1$ and $N_REPEAT = 1000$

a less confident fusion. We propose for the experiment an objective measure of robustness (R). It is computed on Eq.11 as the fraction of the area under the curve of the target hypothesis on the sum of the area under all masses :

$$R = \frac{A(H_i)}{\sum_{\eta=0}^{\mathcal{H}} (A(H_\eta)) + A(H_*) + A(\Omega) + A(\emptyset)} \quad (11)$$

$$A(X) = \int_0^1 m_W(X) d\Delta$$

This equation illustrates that as the robustness of the architecture increases, the decrease of the H_2 curve with respect to Δ diminishes, or its occurrence is delayed. By design, this robustness value falls within the interval $[0, 1]$.

E. Results

The experiment is conducted using the following parameters :

- 3 hypotheses ($\mathcal{H} = 3$).
- Target hypothesis is hypothesis 2 ($H_i = H_2$)
- $N_C = 10$ concordant sources with probabilities: $[0, 1, 0]$.
 $\alpha = 0.5$, $\tau = 0.5$.
- $\Delta_STEP = 0.1$.
- $N_REPEAT = 1000$.

The acceptance and refutation functions were chosen to be mirror images of each other: $ref(x) = acc(-x)$, and selected from the following options:

- $acc(x) = \sin(x)$ for $x \in [-\pi/2, \pi/2]$, denoted as $\sin[-\pi/2, \pi/2]$. This function will give us the same BBF as the original paper [2]
- $acc(x) = x^2$ for $x \in [0, 1]$, denoted as $[0, 1]^2$.
- $acc(x) = -x^2$ for $x \in [-1, 0]$, denoted as $-[-1, 0]^2$.
- $acc(x) = x$ for $x \in [0, 1]$, denoted as $[0, 1]$.
- $acc(x) = -x$ for $x \in [0, 1]$, denoted as $-[0, 1]$.
- $acc(x) = 1$, representing the lower bound, denoted as 1.

The experiment entails conducting iterations for every combination of sources and functions, wherein the robustness is plotted against the number of discordant sources. The goal is to enhance the robustness at each data point. The results are depicted in Fig. 5. The first three lines illustrate the progression of each value within the mass set as the input varies across different setups of our experiment. Meanwhile, the final line represents the plot of all robustness curves as the number of discordant sources increases.

The analysis reveals that the reliability of the fusion architecture declines with an increase in the number of conflicting sources, regardless of the chosen function. This outcome aligns with expectations, as heightened conflict leads to diminished certainty regarding hypothesis 2. Notably, all curves, except for the red one, remain within a reasonable range and do not intersect. Noteworthy is the $[0, 1]$ curve, which exhibits a smaller decline, commencing at a robustness of 0.3829 and concluding at 0.0426. This suggests its potential suitability for high-conflict scenarios. However, the advantages in such contexts diminish in the absence of conflicting sources (with a robustness of 0.3829 compared to 0.5579 for the second-to-last function). Regarding $\sin[-\pi/2, \pi/2]$, the function associated

with formulas from Gruyer's and Magnier's theses performs adequately but is closely matched by $-\pi/2$ and surpassed by $[0, 1]$ and $[0, 1]^2$. Concerning Appriou's set of mass, *App1* and *App2* performs poorly. Especially, *App1* always outputs a mass of 0 on hypothesis. This is due to the architecture used, in which having all $m_\Gamma(H) = 0$ induce null mass on hypothesis. This, expected, allows us to see that our method detects the methods unsuitable for the experiment in its current setup. Lastly, the $[0, 1]^2$ curve (blue) demonstrates superior performance in mitigating noise and discordance effects on the fusion architecture. It outperforms all other functions across all levels of conflicting sources, with a marginal exception at $N_D = 0$ (where $R = 0.7003$ compared to $R = 0.7016$ for $\sin[-\pi/2, \pi/2]$).

V. CONCLUSION

In conclusion, our study has presented a novel approach rooted in belief theory for generating Basic Belief Assignments (BBAs) using a parametric family of functions. This method offers a structured framework for evaluating objective criteria and selecting the most suitable BBA for a given scenario. The key advantage of our method lies in its flexibility and adaptability, allowing for the customization of parameters to optimize data fusion processes. Our experimental results have demonstrated that the fusion architecture's reliability decreases as the number of conflicting sources increases, regardless of the function used. This decrease was expected, as the certainty about hypothesis 2 gets tempered by more and more conflicting sources. However, we observed that certain functions, such as the $[0, 1]^2$ curve, are better suited for minimizing the impact of noise and discordance on the fusion architecture. This function outperformed all others across all numbers of conflicting sources, indicating its effectiveness in generating BBAs that are well-suited to the task at hand. Overall, our study has contributed to the field of belief theory by introducing a new level of adaptability and generality in BBA generation. We believe that this approach has the potential to significantly improve decision-making in uncertain environments and enhance the performance of complex systems. Future research could explore the application of this method in other domains and further investigate its effectiveness in different scenarios.

In future work, there is potential to further iterate on the definition of the Γ family by allowing for multiple extinction coefficients. This extension could enable the creation of multi-inputs BBF, accommodating scenarios with multiple sources of information and corresponding hypotheses. Additionally, exploring alternative representations beyond traditional functions, such as splines with control points, may offer greater flexibility and insight into the dynamics of input data. By leveraging such techniques, researchers can uncover nuanced patterns and relationships, potentially leading to more refined and effective BBF formulations. These advancements hold promise for enhancing the versatility and applicability of BBF in diverse decision-making contexts, paving the way for more sophisticated inference models with broader utility.

Evolution of robustness when discordance increases

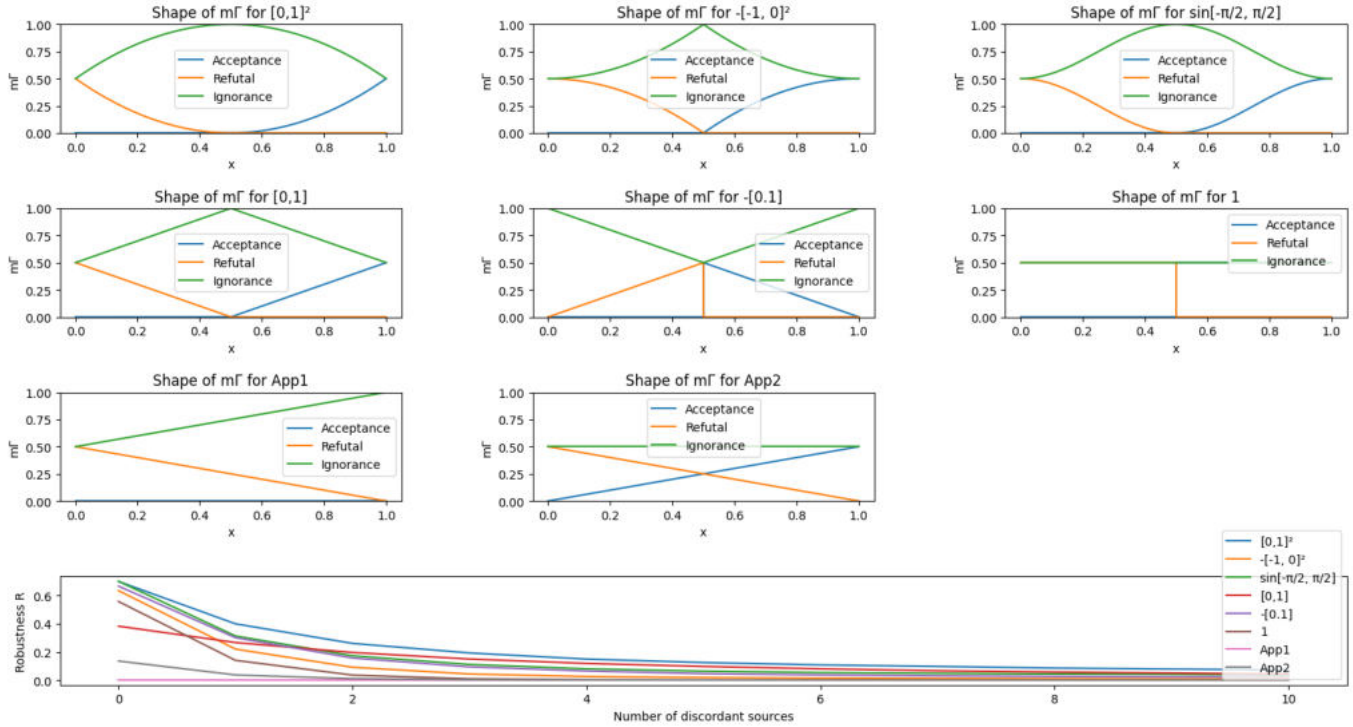


Fig. 5. Results of the experiment with different function shapes

REFERENCES

- [1] A. P. Dempster, "Upper and Lower Probabilities Induced by a Multivalued Mapping," *The Annals of Mathematical Statistics*, vol. 38, no. 2, pp. 325 – 339, 1967. [Online]. Available: <https://doi.org/10.1214/aoms/1177698950>
- [2] D. Gruyer, S. Demmel, V. Magnier, and R. Belaroussi, "Multi-hypotheses tracking using the dempster-shafer theory, application to ambiguous road context," *Information Fusion*, vol. 29, pp. 40–56, 2016. [Online]. Available: <https://www.sciencedirect.com/science/article/pii/S1566253515000962>
- [3] J. Dezert, F. Smarandache, A. Tchamova, and D. Han, "Fast fusion of basic belief assignments defined on a dichotomous frame of discernment," in *2020 IEEE 23rd International Conference on Information Fusion (FUSION)*, 2020, pp. 1–8.
- [4] H. Lee, H. Kwon, R. M. Robinson, W. D. Nothwang, and A. M. Marathe, "Dynamic belief fusion for object detection," in *2016 IEEE Winter Conference on Applications of Computer Vision (WACV)*, 2016, pp. 1–9.
- [5] A. Al-Ani and M. Deriche, "A new technique for combining multiple classifiers using the dempster-shafer theory of evidence," *Journal of Artificial Intelligence Research*, vol. 17, pp. 333–361, 2002.
- [6] Y. Wei and F. Yaowen, "Constructing basic belief assignment from feature data," in *2013 Chinese Automation Congress*, 2013, pp. 605–610.
- [7] W. Jiang, M. Zhuang, C. Xie, and J. Wu, "Sensing attribute weights: A novel basic belief assignment method," *Sensors*, vol. 17, no. 4, 2017. [Online]. Available: <https://www.mdpi.com/1424-8220/17/4/721>
- [8] E. Lefevre, O. Colot, and P. Vannoorenberghe, "Belief function combination and conflict management," *Information Fusion*, vol. 3, no. 2, pp. 149–162, 2002. [Online]. Available: <https://www.sciencedirect.com/science/article/pii/S1566253502000532>
- [9] A. Lepskiy, "Estimation of conflict and decreasing of ignorance in dempster-shafer theory," *Procedia Computer Science*, vol. 17, pp. 1113–1120, 2013.
- [10] J. Li, B. Xie, Y. Jin, Z. Hu, and L. Zhou, "Weighted conflict evidence combination method based on hellinger distance and the belief entropy," *IEEE Access*, vol. 8, pp. 225 507–225 521, 2020.
- [11] W. Fan and F. Xiao, "A new conflict management in evidence theory based on dematel method," *Journal of Sensors*, vol. 2019, pp. 1–12, 2019.
- [12] L. Huang, S. Ruan, and T. Denœux, "Application of belief functions to medical image segmentation: A review," *Information Fusion*, vol. 91, pp. 737–756, 2023. [Online]. Available: <https://www.sciencedirect.com/science/article/pii/S1566253522002184>
- [13] R. P. Srivastava and T. J. Mock, *Belief Functions in Business Decisions*. Springer-Verlag Berlin Heidelberg GmbH, 2002.
- [14] R. P. Srivastava and C. Li, "Risk and reliability formulas for systems security under dempster-shafer theory of belief functions," *Journal of Emerging Technologies in Accounting*, vol. 5, no. 1, pp. 189–219, 2008.
- [15] G. Shafer, *A Mathematical Theory of Evidence*. Princeton University Press, 1976. [Online]. Available: <http://www.jstor.org/stable/j.ctv10vm1qb>
- [16] D. Gruyer and V. Berge-Cherfaoui, "Matching and decision for vehicle tracking in road situation," in *Proceedings 1999 IEEE/RSJ International Conference on Intelligent Robots and Systems. Human and Environment Friendly Robots with High Intelligence and Emotional Quotients (Cat. No.99CH36289)*, vol. 1, 1999, pp. 29–34 vol.1.
- [17] M. Rombaut and V. Cherfaoui, "Decision making in data fusion using dempster-shafer's theory," *IFAC Proceedings Volumes*, vol. 30, no. 7, pp. 339–343, 1997, 3rd IFAC Symposium on Intelligent Components and Instruments For Control Applications 1997 (SICICA '97), Annecy, France, 9–11 June. [Online]. Available: <https://www.sciencedirect.com/science/article/pii/S1474667017432885>
- [18] A. Appriou, *Uncertain Data Aggregation in Classification and Tracking Processes*. Heidelberg: Physica-Verlag HD, 1998, pp. 231–260. [Online]. Available: https://doi.org/10.1007/978-3-7908-1889-5_13